JOURNAL OF MATERIALS SCIENCE 25 (1990) 2975–2984

Influence of alloying elements and heat treatment on impact toughness of chromium steel surface deposits

A. BARBANGELO
Istituto di Meccanica Applicata alle Macchine, Università di Genova, Via all'Opera Pia 15/A, 16145 Genova, Italy

By means of Charpy impact tests, the impact toughness of chromium steels (nominally, 5% and 14% chromium) has been evaluated after the surfacing process and postheating at 350, 450 and 550° C. It has been found that impact toughness is primarily affected by the ratio between the nickel and chromium contents of the filler metals. The amount of energy required for impact fracture increases as the nickel to chromium ratio increases from 0.01 to 0.29. A metallographic analysis has shown that the nickel : chromium parameter affects the impact toughness, in that a different microstructure is obtained as this ratio varies. A marked susceptibility to temper embrittlement has been noticed for all types of filler metals examined. All materials are embrittled by postheating at 450° C; for some of them, temper embrittlement also occurs at postheating temperatures of 550° C. A decrease in toughness results in a larger number of brittle-fracture regions on the impact fracture surfaces. The brittle regions were observed to proceed primarily by a cleavage rupture mechanism.

1. Introduction

The surfacing process is the deposition of filler metals on a metal surface by welding, in order to obtain both the restoration of deteriorated industrial equipment and the fabrication of components with composite structures. The main applications of this technique concern those components which are utilized under such conditions so as to require either their frequent replacement or the use of very costly materials.

In this area, chromium steels are interesting for both their oxidation resistance and good mechanical characteristics. In particular, in the presence of suitable carbide-forming elements, these steels can reach very high hardness values, with a consequent high abrasion resistance.

Nevertheless, such hard surfacing materials often exhibit a poor notch toughness, thus running the risk of catastrophic fractures in service. Many factors can contribute to losses in the toughness of these surfacing materials. An unfavourable distribution of hard carbides is possible, in that the microstructures of surfacing materials are determined by the unusual conditions under which solidification has taken place. The possible presence of hydrogen inside a material, with consequent embrittlement, is a non-negligible factor, since it is a typical risk of the welding process. Moreover, these materials can contain, as carbide-forming elements, vanadium and niobium, which are reversible traps for hydrogen [1]. Many of the chromium steels utilized in the surfacing process produce a martensitic weld structure, with possible tempered martensite embrittlement and consequent drop-off in toughness [2, 3]. It is worth noting that the surfacing technique involves a short temper, in that, in order to obtain high thickness values, the multiple-pass weld technique is used, which induces various thermal variations in deposited material. Furthermore, temper embrittlement increases the hydrogen embrittlement susceptibility due to a cooperative relation between the two types of embrittlement [2, 4, 5].

The purpose of the present investigation is to determine the chemical composition and the postheating temperature that make it possible to obtain a good impact toughness for chromium steels as surfacing filler materials, without affecting their hardness characteristics. The materials examined are two sets of commercial fillers of self-hardening steels; the two sets differ in the chromium content (nominal chromium contents: 5% and 14%), and each set consists of various steels with different contents of the other alloying elements. The tempering temperature values used are: 350, 450 and 550° C. Higher temperatures have not been considered, as they cause a notable decrease in hardness. High hardness is a basic requirement for the employment of these materials.

Toughness values have been determined by means of Charpy impact tests on as-deposited and postheat-treated materials. The microstructures of the materials have also been determined, and a fractographic analysis of the impact fracture surfaces has been carried out.

2. Experimental

The materials examined in this investigation are a set

0022–2461/90 $03.00 + .12

TABLE I Chemical compositions of the deposits examined (wt %)

Deposit No.	C	Si	Mn	Ni	Cr	Mo	W	V	Nb
1	0.22	0.54	1.83	0.83	4.86	1.33	0.95	–	0.59
2	0.17	0.97	0.79	1.20	4.88	2.13	2.05	–	–
3	0.21	0.36	0.53	0.47	5.10	1.47	1.05	–	0.80
4	0.36	0.39	0.25	0.94	5.51	2.37	2.42	–	2.05
5	0.29	0.26	0.36	1.12	5.59	1.95	2.00	–	–
6	0.24	0.16	0.26	1.18	5.64	1.06	1.04	0.33	–
7	0.26	0.37	0.59	0.84	5.88	1.47	0.91	–	1.01
8	0.23	0.75	0.47	1.60	12.61	1.18	0.88	–	0.80
9	0.30	0.89	0.54	0.97	13.15	0.95	0.96	–	0.59
10	0.31	0.39	0.35	1.02	13.40	0.96	0.96	–	0.72
11	0.36	0.74	0.55	1.07	13.64	1.02	0.45	0.30	–
12	0.38	0.66	0.47	1.02	13.95	0.97	0.38	–	–
13	0.31	0.88	0.90	0.47	14.20	1.34	–	–	–
14	0.14	0.59	0.46	4.11	14.30	0.92	–	–	–
15	0.07	1.06	1.00	4.06	14.30	0.99	–	–	–
16	0.19	1.25	1.16	0.12	14.30	1.01	–	–	–
17	0.40	0.36	0.35	1.08	14.56	0.99	0.44	0.33	–
18	0.31	0.56	0.58	0.12	14.70	1.08	–	–	–
19	0.42	0.38	0.46	0.75	15.17	1.01	0.39	–	0.38

of surfacing chromium steels, both as-deposited and after postheating.

Deposits were performed by submerged arc welding, using 19 commercial fillers of self-hardening chromium steels. The nominal chromium content of seven of these electrodes was equal to 5%, and that of the other 12 electrodes was equal to 14%; the contents of the other alloying elements varied from electrode to electrode (see Table I). After surfacing, four blanks of each type of material were examined; three blanks were subjected to a different postheating temperature for a period of 8 h; the first blank was tempered at 350° C, the second at 450° C, and the third at 550° C. The materials were denoted by a number (from 1 to 19), which increased according to the actual chromium content.

The postheat treatments were denoted as follows: A for the as-deposited material, B for the material tempered at 350° C, C for the material tempered at 450° C, and D for the material tempered at 550° C.

The chemical compositions of the deposits are given in Table I. In addition to the elements listed in the table, all materials considered in this study contained hydrogen whose presence was detected by means of fatigue crack growth tests carried out on the materials [6]. However, the hydrogen percentages were not high enough to be measured by the standard analytical technique.

The hardness values measured for the various surfacing steels, as deposited and after tempering, are given in Table II.

From such deposits, in the various heat-treatment states, specimens for the impact toughness tests were obtained whose dimensions were: 10 mm height, 10 mm width, and 15 mm length.

The specimens were drawn in a longitudinal direction so that the notches (U-shaped and 2 mm deep) were perpendicular to the weld beads; it is in this direction that fractures usually occur in service. The Charpy impact tests (20 for each material, i.e. 5 for each heat treatment) were performed at a temperature of 20° C. The fractured specimens were subjected to fractographic examination in the scanning electron microscope (SEM) and to metallographic analysis. In order to clarify the various components of the microstructures, different etchants were employed in the metallographic analysis: nital 5% (5 ml HNO_3–95 ml ethanol), acid hydrogen peroxide (35 ml HCl–65 ml ethanol–7 drops H_2O_2 30%) and mixed acids (15 ml HCl–15 ml HNO_3–10 ml acetic acid) for general structures; and Murakami's reagent (10 g $K_3Fe(CN)_6$–10 g KOH–100 ml water) for carbide particles.

3. Results and discussion

3.1. Impact toughness

The values of the impact toughness, K, obtained for the steels examined, in the as-deposited state and after postheating at temperatures 350, 450 and 550° C, are given in Table III.

TABLE II Brinell hardness values for the surfacing steels, as deposited and after postheating: A, as deposited; B, postheated at 350° C; C, postheated at 450° C, and D, postheated at 550° C

Deposit No.	Brinnell hardness			
	A	B	C	D
1	430	415	430	302
2	423	415	430	375
3	392	415	445	331
4	444	461	471	320
5	453	477	496	534
6	514	495	461	388
7	460	445	445	330
8	437	435	477	350
9	555	514	495	477
10	534	461	477	341
11	477	461	495	360
12	477	445	461	320
13	514	477	514	445
14	394	363	375	320
15	415	388	408	321
16	434	388	401	277
17	430	415	477	320
18	475	472	472	461
19	514	477	505	340

TABLE III Values of the impact toughness, K, for the surfacing steels: A, as deposited; B, postheated at 350° C; C, postheated at 450° C, and D, postheated at 550° C

Deposit No.	K(J cm^{-2})			
	A	B	C	D
1	11.8	11.0	9.6	10.2
2	29.0	32.0	31.0	24.0
3	9.0	7.4	5.8	8.0
4	10.2	10.2	6.8	10.2
5	12.8	14.2	12.2	10.0
6	20.0	20.0	11.8	31.0
7	10.8	11.8	8.4	7.8
8	9.4	9.6	7.0	10.7
9	6.0	8.0	5.0	12.5
10	6.0	8.0	7.0	7.0
11	6.2	6.6	4.8	12.4
12	5.4	6.4	5.0	11.0
13	5.4	7.0	4.6	19.0
14	23.6	34.6	26.5	41.3
15	32.0	38.0	38.0	34.4
16	5.0	6.2	4.6	14.0
17	6.6	8.0	5.0	10.8
18	4.2	6.6	6.2	5.2
19	5.2	7.6	6.2	13.7

The data in Table III point out that the chromium content does not directly affect the impact toughness of the materials; in fact, no marked difference can be seen between the behaviour of medium-chromium steels (from 1 to 7) and stainless steels (from 8 to 19).

Instead a comparison of the results in terms of the various alloying elements shows a dependence of the Charpy toughness on the ratio between the weight percent nickel and chromium contents of a material. Fig. 1 shows the behaviour of impact toughness as a function of the nickel to chromium ratios of the deposits examined, for the four heat treatment states. Examination of graphs a, b and c shows that, under the heat treatment conditions: as-deposited, postheat at 350° C, postheat at 450° C, the toughness of deposits improves as the ratio of the nickel content to the chromium content increases. The absolute chromium content does not directly affect the toughness of a material; for instance, for deposits 7 and 8, the chromium content ranges from 5.88% to 12.61%, but their toughness values turn out to be close, as the nickel to chromium ratios are also close (0.14 and 0.13 respectively). Instead, deposits 15 and 16, despite their equal chromium content (14.30%), exhibit an extremely different impact behaviour, their nickel to chromium ratios being equal to 0.28 and 0.01, respectively. Analogously, the absolute nickel content does not affect toughness directly; deposits 7 and 8 exhibit a similar impact behaviour, although the latter contains twice as much nickel as the former. Moreover, a 1.20% nickel content is enough for deposit 2 to retain high toughness values (about 30 J cm^{-2} for the three heat-treatment states), while a 1.60% nickel content is not enough for deposit 8 (toughness values lower than 10 J cm^{-2}).

The other alloying elements, at the same nickel to chromium ratio, do not seem to have any definite effects on impact toughness. Higher concentrations of carbon and carbide-forming elements seem to have detrimental effects on impact toughness, as can be noticed by comparing the behaviour of deposit 1 with that of deposit 4, the behaviour of deposit 5 with that of deposit 6, and the behaviour of deposit 14 with that of deposit 15. Instead, a higher carbon content is no more detrimental for deposit 18 than for deposit 16, and a higher content of carbide-forming elements of deposit 2 does not involve a worse impact behaviour than deposit 14.

The presence of niobium was found to decrease the impact toughness values of hot-worked HSLA steels [7] and of HSLA and high tensile (HT) steels after the welding process [8, 9], but it turned out to be beneficial for hot-worked low-alloyed steels [10]. In the present case, niobium does not seem to have any specific effect on the toughness values of the deposits examined.

Fig. 1d, which refers to deposits postheated at 550° C, shows a considerable scatter in data. To explain this fact, which partially invalidates the direct influence of the nickel to chromium ratio on impact toughness, it is necessary to examine the variations in toughness as the postheat temperature rises. The data in Table III point out two different types of behaviour, as shown in Fig. 2. The data related to each material are joined by broken lines, which do not represent the impact toughness behaviour at intermediate temperatures, but are drawn for a better visualization of the data obtained for the same type of deposit. For both types of behaviour, the toughness of the deposits postheated at 350° C increases, as compared with the as-deposited condition, and then it decreases when the deposits are postheated at 450° C. If the postheat temperature rises to 550° C, the behaviour of the materials differs; for some materials (Fig. 2a), the impact toughness increases, while for other materials (Fig. 2b), it decreases further.

The toughness degradation over a given range of heat-treatment temperatures is called temper embrittlement or tempered martensite embrittlement, and can be ascribed to various factors. After investigating martensitic stainless steels, Banerjee *et al.* [11] postulated an embrittlement mechanism based on the transformation of M_3C carbides into $M_{23}C_6$ carbides, as the tempering temperature increases. The occurrence of embrittlement after temper may also be due to the segregation of residual impurities, such as phosphorus, antimony, tin and arsenic [5, 12, 13] on the grain boundaries. The phenomenon may also be caused by the instability of retained austenite, which decomposes to form carbides [3].

The drop-off in toughness caused by temper embrittlement in the materials examined can be made more evident by the presence of trapped hydrogen, even though the concentration of diffusible hydrogen decreases with postheating, in that the susceptibility of a steel to hydrogen embrittlement is markedly increased if the steel is tempered within the temper-embrittlement range [2, 4, 5].

The occurrence of temper embrittlement during postheating of the deposits indicates that the short temper that takes place automatically during the multiple-pass process is not sufficient for the phenomenon to occur completely.

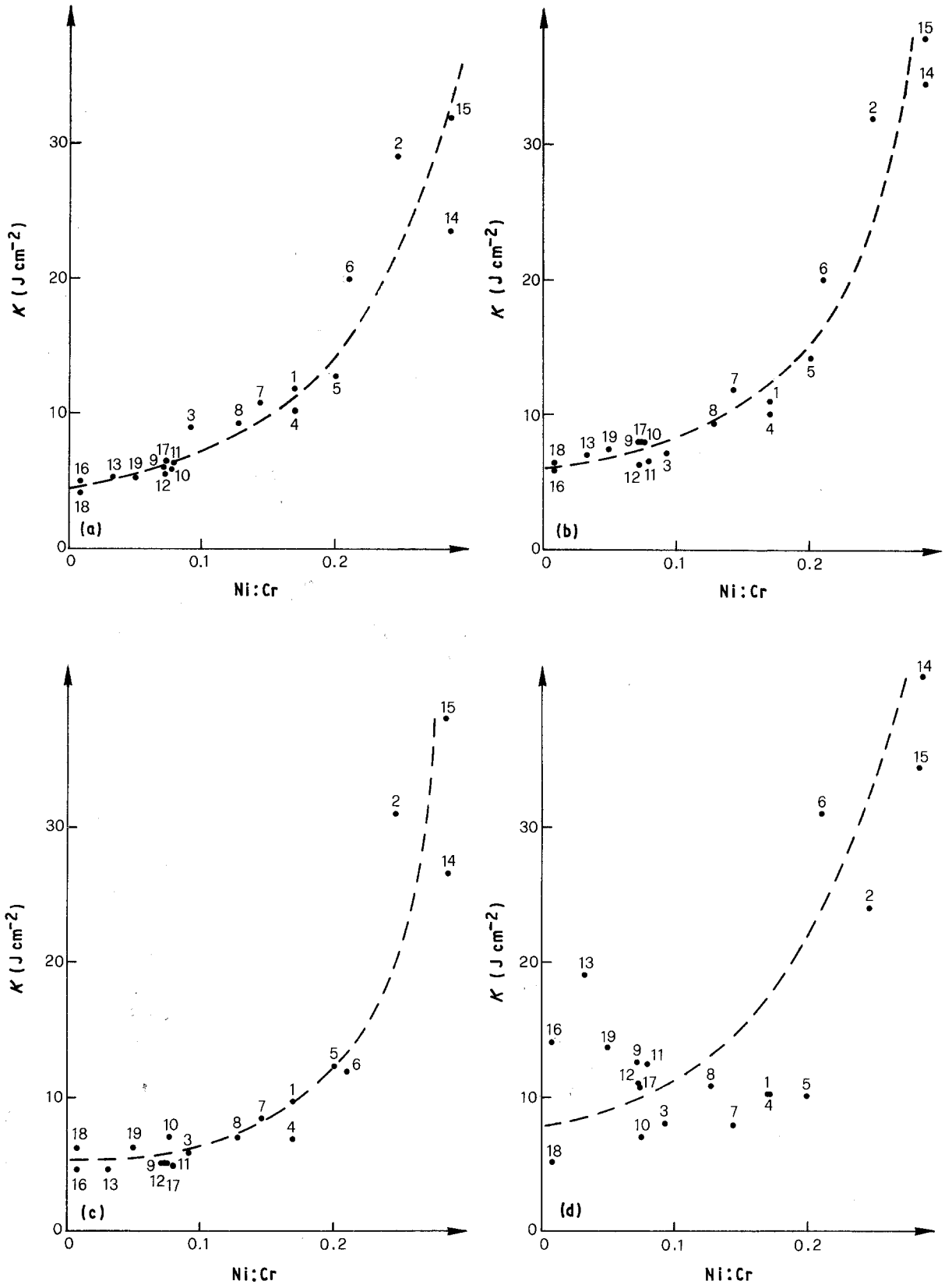

Figure 1 Impact toughness, K, as a function of the ratio between the nickel and chromium weight contents (Ni to Cr) of the materials: (a) as-deposited, (b) postheated at 350° C, (c) postheated at 450° C, (d) postheated at 550° C.

For all the materials under examination, the temper embrittlement range is located above 350° C; for some of them, the temperature of 550° C is inside the embrittlement range, whereas for the others, this temperature is outside the range. The fact that a temperature of 550° C can be higher or lower than the extreme value of this range leads to the differentiation of the behaviour presented in Fig. 2, and causes the scatter in data shown in Fig. 1d.

The increase or decrease in the impact toughness of the materials postheated at 550° C (as compared with those postheated at 450° C) may not be indicative of a different behaviour of the materials; in fact, above a temperature range causing embrittlement, an increase

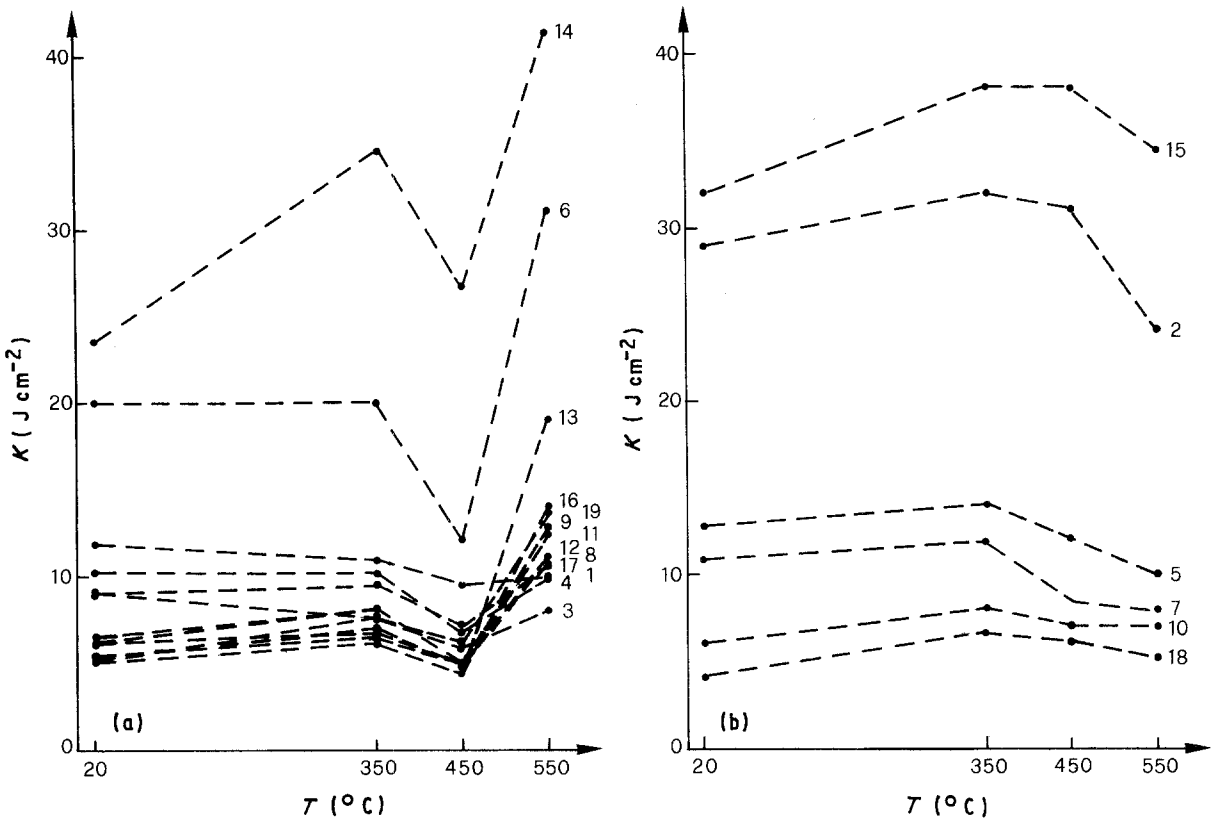

Figure 2 Variatons in impact toughness, K, with postheating temperature, T: (a) materials which exhibit an increase in toughness when the postheating temperature rises from 450° C to 550° C, (b) materials which exhibit a decrease in toughness when the postheating temperature rises from 450° C to 550° C.

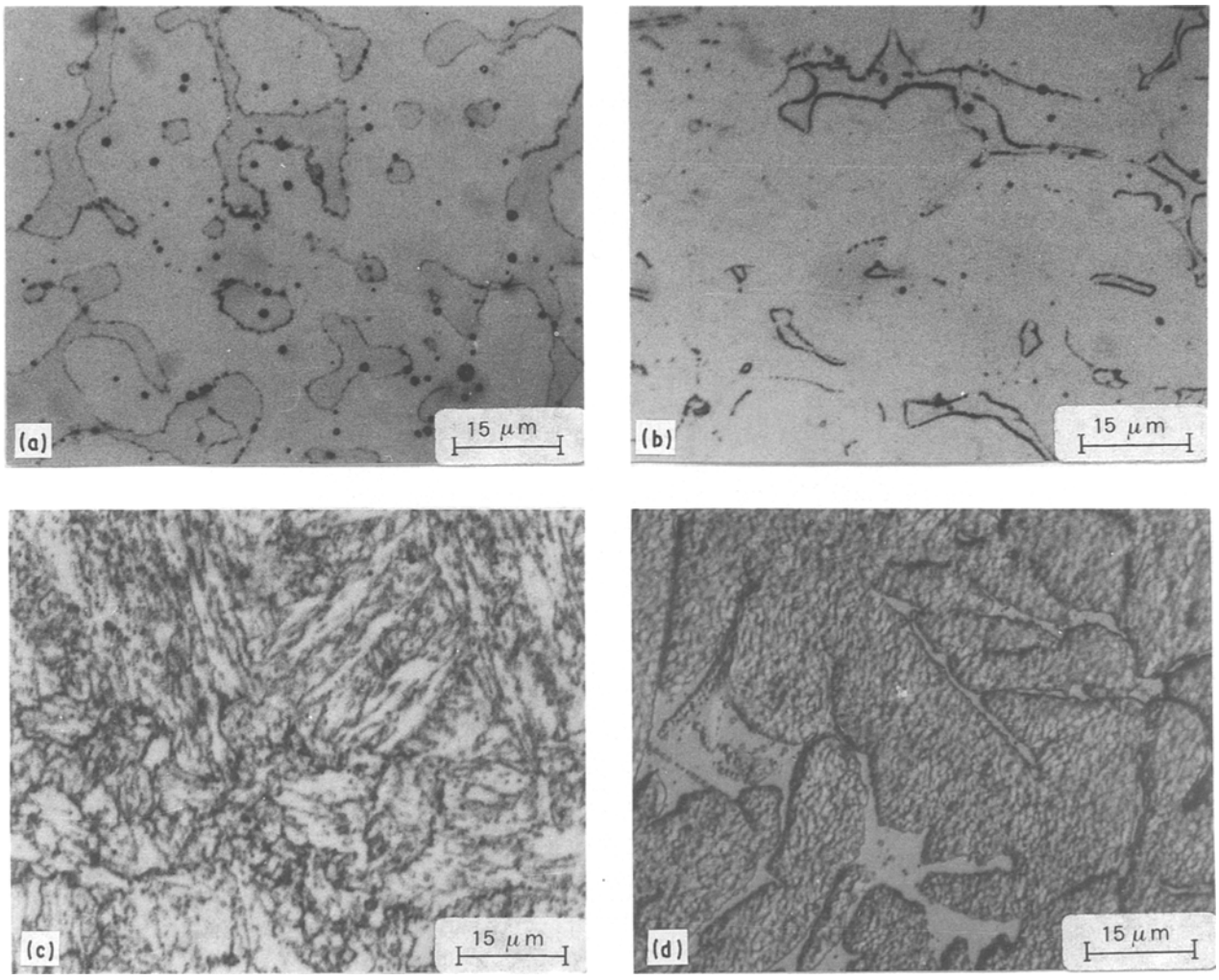

Figure 3 Microstructures of deposits postheated at 350° C: (a) deposit 16, (b) deposit 10, (c) deposit 1, (d) deposit 15.

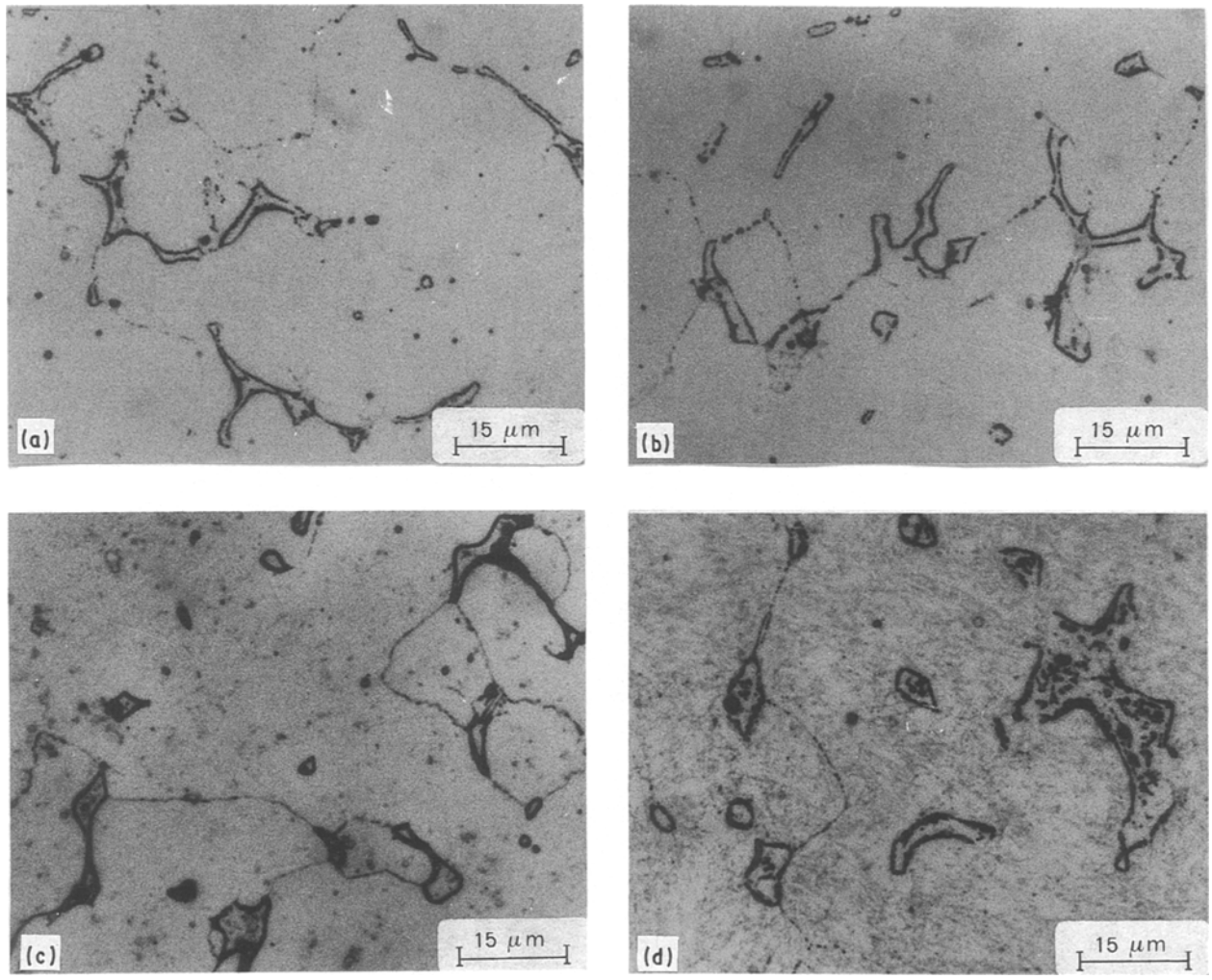

Figure 4 Microstructures of deposit 19: (a) as-deposited, (b) postheated at 350° C, (c) postheated at 450° C, (d) postheated at 550° C.

in toughness is generally very sudden; a slight variation in the range width is enough to obtain entirely different toughness values.

3.2. Metallography

The microstructural analysis of the sections of material taken from tested impact specimens has pointed out three different types of structure. The structure of filler materials 3, 8, 9, 10, 11, 12, 13, 16, 17, 18 and 19 consists of islands of ferrite in a martensite matrix; the structure of filler metals 1, 4, 5 and 7 is a fully martensitic matrix; in the structure of filler metals 2, 6, 14 and 15, some austenite appears in the martensite matrix.

The above microstructures are different from those which could have been predicted by utilizing the constitution diagram for deposited weld metals proposed by Schaeffler [14]. In the present case, the different microstructures can be ascribed to the unusually high concentration of carbide-forming elements in the steels examined. In the Schaeffler diagram, the microstructure is dependent on the equivalent nickel content and on the equivalent chromium content of the materials considered, whereas the microstructure of the materials under examination turns out to depend on the nickel to chromium weight ratio.

As the nickel to chromium ratio increases, the steel structure changes from a network of ferrite in a martensite matrix to a martensite matrix in which the ferrite content is lower, and then (when the nickel to chromium ratio reaches values ranging from 0.14 to 0.20) to a fully martensitic matrix. A further increase in the nickel to chromium ratio causes the martensitic matrix to contain retained austenite.

Examples of the types of microstructure obtained by the same heat treatment are given in Fig. 3. Fig. 3a, which refers to deposit 16 (Ni : Cr = 0.01), shows islands of ferrite (dark grey) in martensite; shows the presence of globular carbides (dark spots), which appear both dispersed in the two phases and located at the martensite–ferrite interface. Fig. 3b, which refers to deposit 10 (Ni : Cr = 0.08), presents a similar structure to that in Fig. 3a, but the ferrite islands are smaller. For deposit 1 (Ni : Cr = 0.17), Fig. 3c shows an entirely martensitic structure with dispersed carbides. The structure in Fig. 3d, which refers to deposit 15 (Ni : Cr = 0.28), consists of a fine network of austenite (light grey) in martensite; the presence of globular carbides is shown by small dark circles inside austenite and at the martensite to austenite interface.

The fact that both the microstructure and the Charpy energy of the materials examined are dependent on the nickel to chromium ratio demonstrates that the microstructure is the main parameter in the control of impact toughness. A martensitic-ferritic microstructure is more detrimental for impact toughness than an entirely martensitic structure; the highest

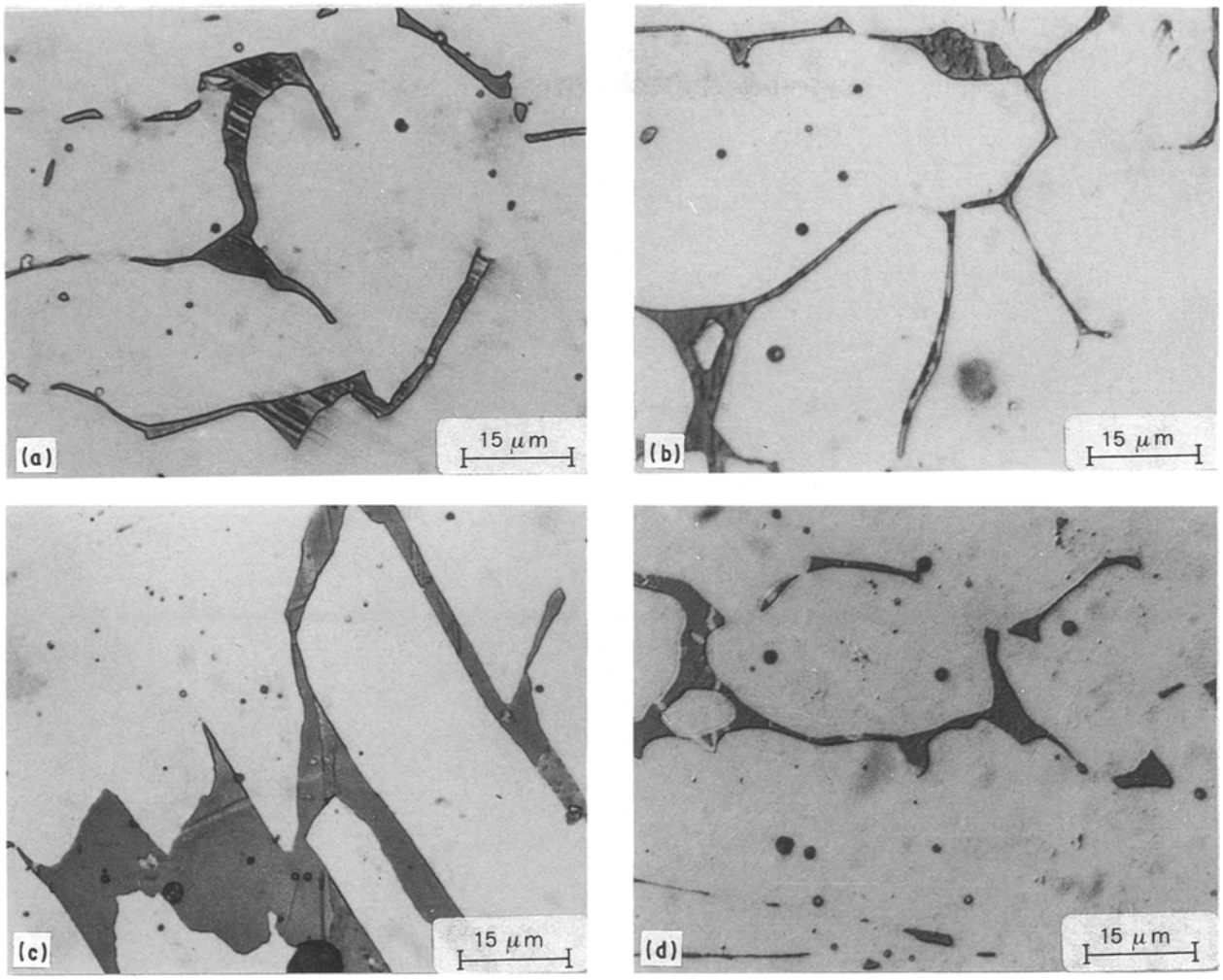

Figure 5 Microstructures of deposit 15: (a) as-deposited, (b) postheated at 350° C, (c) postheated at 450° C, (d) postheated at 550° C.

toughness values are measured in a martensitic–austenitic microstructure.

The detrimental effect of ferrite on the ductility of a material, particularly in the presence of hydrogen (as in the present case), has been reported by various authors. Hayden and Floreen [15] studied the properties of six martensitic–ferritic stainless steels, with a microduplex structure and a ferrite content ranging from 8.4 to 100%, and found a decrease in impact toughness as the ferrite content of the steels increased.

In the presence of hydrogen, the deleterious effect of ferrite can be even more noticeable; in fact, Sudarshan *et al.* [16] report that martensitic–ferritic steels are particularly sensitive to hydrogen embrittlement, and that a decrease in ductility can be ascribed to a weakening of the martensite–ferrite interface. An analogous effect of the ferrite content has been observed by Blumfield *et al.* [17] on deposits of austentitic–ferritic steel, in the probable presence of hydrogen: by increasing the nickel content of welding electrodes (with a consequent increase in the austenitic phase to the prejudice of the ferritic one), a significant increase in the toughness values of the deposits occurs.

A beneficial effect of the presence of retained austenite (provided that it is stable) on toughness has been reported by Thomas [3] for martensitic steels.

As the postheating conditions vary, the distribution of the phases in the structure of a material remains the same; instead, the concentration of carbide particles changes. A 450° C postheating causes secondary carbides to precipitate; this phenomenon is more significant in the case of 550° C postheating. An example of a typical series of micrographs, obtained by different postheatings for each material, is presented in Fig. 4. Micrographs 4a, 4b, 4c and 4d refer to deposit 19 under the following heat-treatment conditions: as-deposited, postheated at 350° C, postheated at 450° C, and postheated at 550° C, respectively. They show a martensitic–ferritic matrix, in which carbides are dispersed in the two phases, located at the martensitic–ferrite interface, and aligned along the primary austenitic grain boundary. Unlike Figs 4a and 4b, Fig. 4c points out the presence of secondary carbides (small spots which are less dark than primary carbides), and Fig. 4d shows an increase in the dimensions of carbides, due to coalescence.

For martensitic–austenitic structures, Thomas [3] suggests, as previously mentioned, that temper embrittlement may be due to austenite transformation. In the materials examined, the large retained austenite grains, when present, keep stable at the postheating temperatures considered, as can be seen from the micrographs in Fig. 5 related to deposit 15, under the four heat-treatment conditions.

3.3. Fractography

A fractographic analysis of the fracture surfaces of the Charpy specimens shows fracture morphologies

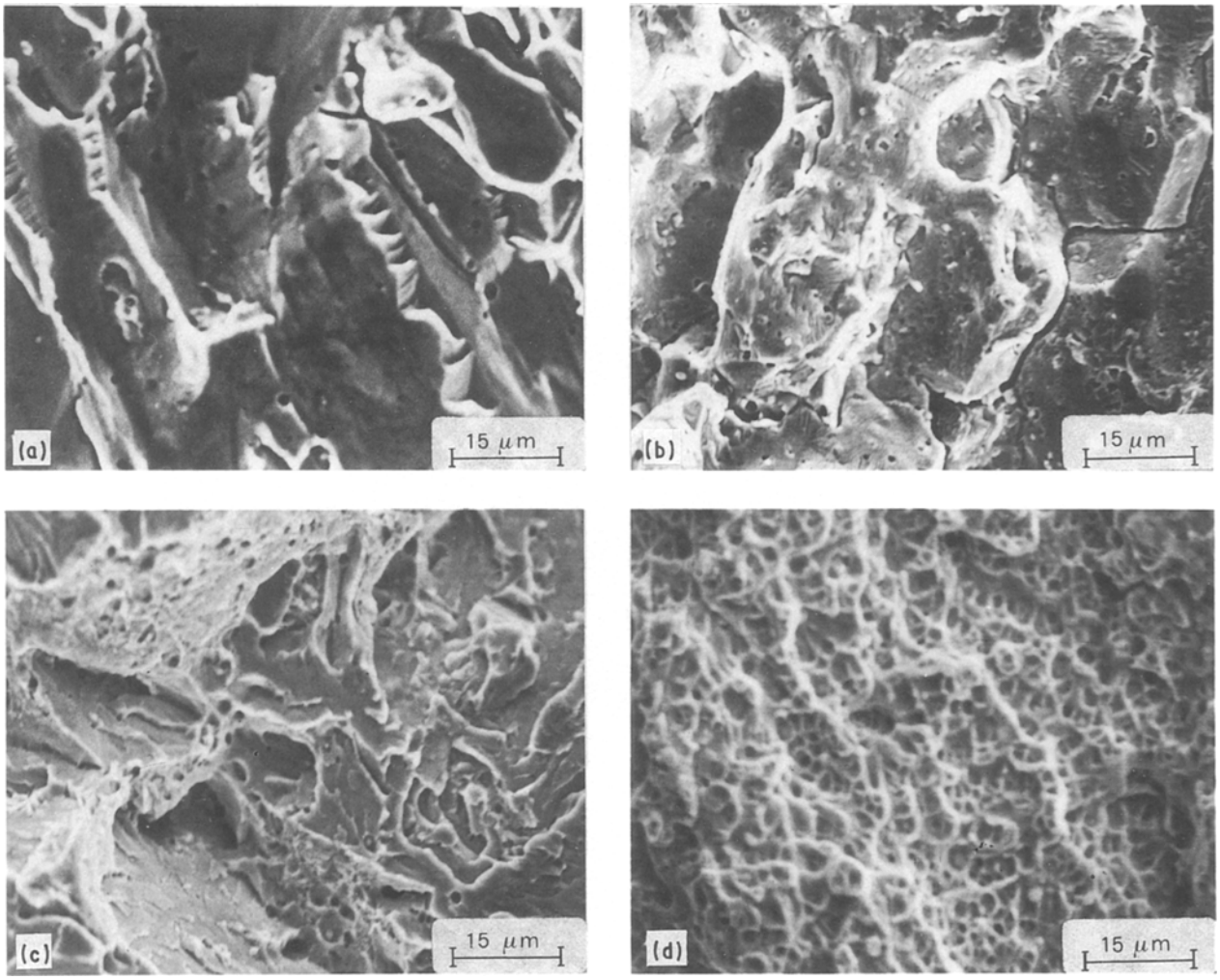

Figure 6 Fractographs of impact fracture surfaces of deposits postheated at 350° C: (a) deposit 18, (b) deposit 13, (c) deposit 7, (d) deposit 14.

ranging from entirely brittle to ductile–brittle, and to entirely ductile. The fracture mechanism of each material is strictly related to the energy absorbed in the impact test.

The specimens that exhibited impact toughness values lower than 8 J cm^{-2} show an almost completely brittle fracture morphology; when the fracture occurred with an energy absorption ranging between 8 and 32 J cm^{-2}, the morphology was ductile–brittle.

For toughness values higher than 32 J cm^{-2}, the fracture surfaces appear almost completely ductile. The ductile fracture zones observed were due to microvoid coalescence, while the brittle fracture zones consist, in most cases, of cleavages with rare intergranular ruptures; only deposits 13 and 9 exhibit brittle fractures that are mainly intergranular.

Examples of the types of fracture morphology observed are given in Fig. 6. The four fractographs refer to materials postheated at 350° C. In Fig. 6a, deposit 18, fractured with an energy absorption of 6.6 J cm^{-2}, exhibits an almost completely brittle fracture surface, largely made up of cleavage facets. In Fig. 6b, deposit 13, which, according to impact tests, is characterized by a comparable toughness (7.0 J cm^{-2}), exhibits an entirely brittle fracture surface, although, in this case, the fracture shows separate grain facets. Fig. 6c which refers to deposit 7 with a toughness of 11.8 J cm^{-2}, shows a fracture surface characterized by a ductile–brittle morphology: the surface contains many cleavage facets with intervening regions of fine dimples. Fig. 6d, which refers to deposit 14 with a toughness of 34 J cm^{-2}, shows that the fracture of the material has occurred almost completely by microvoid coalescence. Under different heat treatment conditions, a given material exhibits similar fracture morphologies, although the development of the ratio between the percentages of ductile fracture regions and those of brittle fracture regions is consistent with the change in impact toughness. For instance, for deposit 2 (which toughness, under the conditions: as-deposited, postheated at 350° C, postheated at 450° C and postheated at 550° C, is equal to 29 J cm^{-2}, 32 J cm^{-2}, 31 J cm^{-2} and 24 J cm^{-2}, respectively), all fracture surfaces show (Figs 7a to 7d) facets that resulted from a combination of large dimples and transcrystalline cleavage. Fig. 7 points out how the fracture surface of the material postheated at 350° C (Fig. 7b), which is characterized by the highest impact energy absorption, exhibits the smallest number of cleavage zones; in comparison, the fracture surface of the material postheated at 550° C (Fig. 7d), which is characterized by the lowest energy absorption, exhibits the highest concentration of brittle fracture zones.

Both the fact that most of the brittle fractures observed occurred by cleavage and the fact that the morphology of the fracture surfaces of the same type

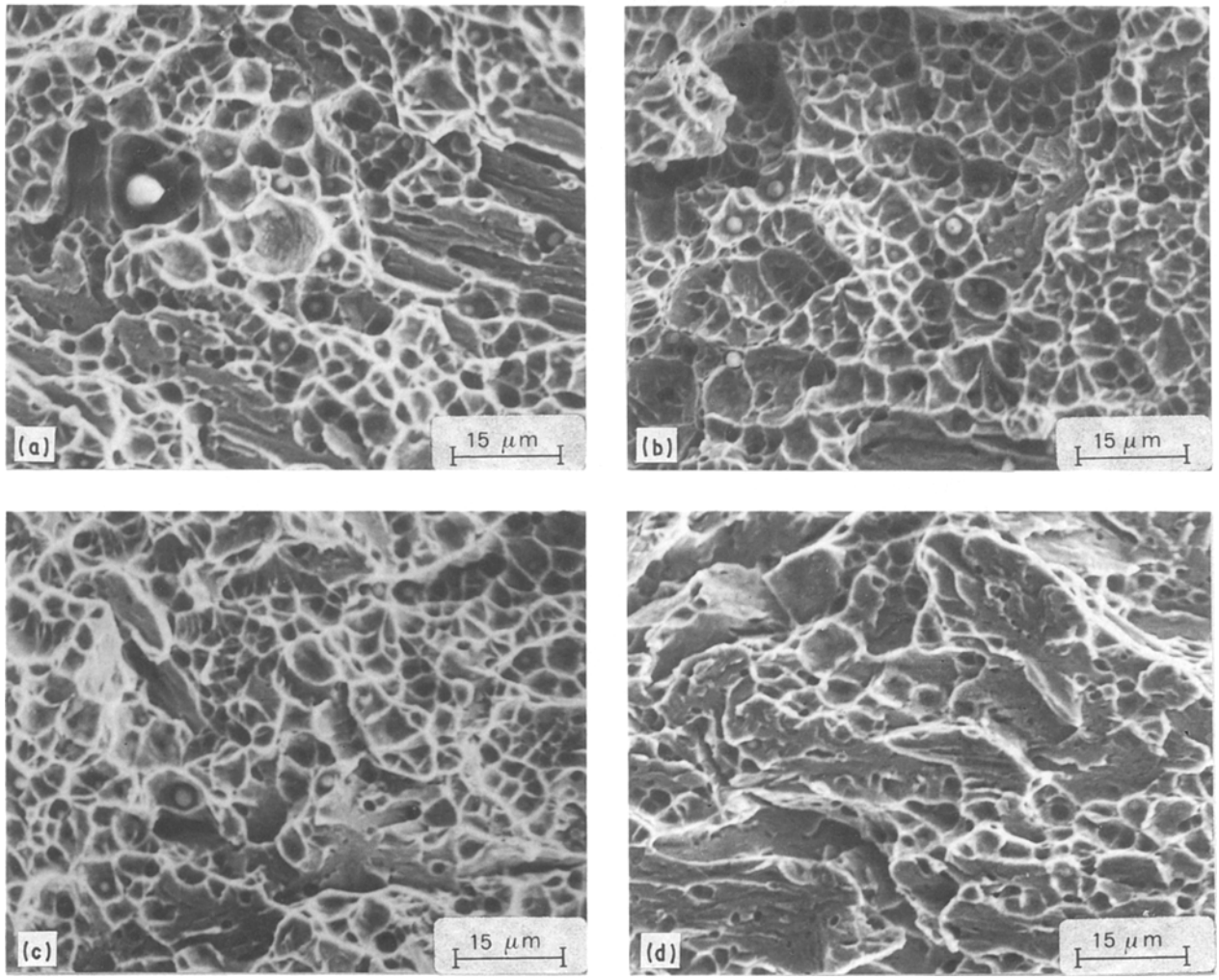

Figure 7 Fractographs of impact fracture surfaces of deposit 2: (a) as-deposited, (b) postheated at 350° C, (c) postheated at 450° C, (d) postheated at 550° C.

of material does not vary with the postheating temperature lead, in general, to exclude that, for the present materials, embrittlement may be due to segregation of impurities on the grain boundaries. In fact, this type of embrittlement involves a mechanism of intergranular fracture.

An analogous low susceptibility to grain-boundary segregation embrittlement has been observed in chromium steels, subjected to a traditional solidification process, when their nickel content is low or zero [18, 19].

Both the fact that the decrease in toughness caused by temper results in a larger number of cleavage zones for all types of microstructures and the fact that the large retained austenite grains, when present, are stable on tempering, lead to exclude that the primary cause of temper embrittlement may be a segregation phenomenon or a transformation of the austenite phase. The observed susceptibility to temper embrittlement could be ascribed, as suggested by Banerjee [11], to an increase and blocking of dislocations caused by dissolution of M_3C carbides, with a contemporary precipitation of $M_{23}C_6$ carbides.

4. Conclusions

The study of the impact fracture behaviour of chromium steels, as surfacing filler metals, leads to the following concluding remarks.

(1) The impact toughness of deposits is affected by the ratio between the nickel and chromium contents because this ratio affects the microstructure resulting from the surfacing process. Over the range of the nickel to chromium ratio from 0.01 to 0.29, the highest impact toughness values correspond to the highest values of this parameter, which are associated with a martensitic–austenitic structure. If surface deposits do not require stainless properties, the choice of steels with a lower chromium content would make it possible to obtain a high impact toughness with a lower nickel content.

(2) Postheating at 450° C causes temper embrittlement in all the materials examined, with a consequent decrease in the toughness values. Some of these materials are also embrittled by postheating at 550° C. A fractographic analysis has pointed out that the brittle fracture zones on the fracture surfaces are mostly due to cleavage and not to grain boundary decohesions; as a consequence, for most of the materials, an impurity-induced embrittlement is excluded as a cause of brittle fracture. Therefore, a higher degree of purity in the welding alloys would not increase impact toughness. The most likely cause of brittleness following postheating lies in transformation of carbides. However carbides cannot be eliminated in the materials examined, for which high hardness is a primary feature.

Acknowledgement

The author is grateful to Dr A. Conte of Italsider S.p.A.(Savona) for supplying the materials and performing the Charpy tests.

References

1. G. M. PRESSOUYRE, J. DOLLET and B. VIELLARBARON, *Mém. Et. Sci. Rev. Mét.* April (1982) 161.
2. G. M. GORDON, in "Stress Corrosion Cracking and Hydrogen Embrittlement of Iron Base Alloys" (N.A.C.E., Houston, Texas, 1977) p. 893.
3. G. THOMAS, *Metall. Trans.* **9A** (1978) 439.
4. K. YOSHINO and C. J. McMAHON, Jr., *Metall. Trans.* **5** (1974) 363.
5. S. K. BANERJI, C. J. McMAHON, Jr and H. C. FENG, *Metall. Trans.* **9A** (1978) 237.
6. A. BARBANGELO, unpublished research (1989).
7. L. F. PORTER, in "Encyclopedia of Materials Science and Engineering" (Pergamon Press, Oxford, 1986) p. 2157.
8. N. E. HANNERZ, *Welding J.* May (1975) 162s.
9. N. E. HANNERZ, in "Welding of HSLA (Microalloyed)" Structural Steels International Conference (A.S.M., Metals Park, Ohio, 1976) p. 365.
10. A. S. TETELMAN and A. J. McEVILY, in "Fracture of Structural Materials" (John Wiley, New York, 1967) p. 514.
11. B. R. BANERJEE, J. J. HAUSER and J. M. CAPENOS, in ASTM STP 369 (American Society for Testing and Materials, Philadelphia, 1969) p. 291.
12. C. L. BRIANT and S. K. BANERJI, *Metall. Trans.* **10A** (1979) 123.
13. J. R. RELLICK and C. J. McMAHON, Jr, *ibid.* **5** (1974) 2439.
14. A. L. SCHAEFFLER, *Met. Prog.* **56** (1949) 680.
15. H. W. HAYDEN and S. FLOREEN, *Metall. Trans.* **1** (1970) 1955.
16. T. S. SUDARSHAN *et al.*, *ASME J. Engng. Mater. Technol.* **107** (1985) 343.
17. D. BLUMFIELD, G. A. CLARK and P. GUHA, *Met. Construction* May (1981) 269.
18. T. WADA and W. C. HAGEL, *Metall. Trans.* **9A** (1978) 691.
19. C. J. McMAHON, Jr, D. H. GENTNER and A. H. UCISIK, *ASME J. Engng Mater. Technol.* **106** (1984) 66.

Received 16 February
and accepted 24 August 1989